

Broad-band fluorescent all-fiber source based on microstructured optical fibers

Veselin Vladev,¹ Tinko Eftimov¹, Wojtek Bock²

¹ Faculty of Physics, Plovdiv University, Plovdiv, Bulgaria,

² Centre de recherche en Photonique, Département d'informatique et d'ingénierie, Université du Québec en Outaouais, Gatineau, Québec, Canada

Received March 25, 2015; accepted June 29, 2015; published June 30, 2015

Abstract—The present work demonstrates a miniature all-fiber fiber-optic fluorescence source on the basis of organic dyes. A capillary of fused silica has been used to keep the Rhodamine 6G dissolved in glycerine at one end of which a tapered optical fiber is inserted to receive the useful signal. The fluorescence medium is side excited with CW laser radiation at 532 nm by a fiber taper. The functioning of the system is demonstrated using a conventional optical fiber, photonic crystal fiber and a hollow-core fiber.

The development of fiber optic gratings stimulated the development of both telecommunications and fiber-optic sensors. Long period gratings (LPG) having a pitch from 100 μm to 800 μm are easy to fabricate and are used in temperature, strain and refractive index sensors initially demonstrated with conventional fibers [1].

Since their first appearance, the microstructured optical fibers (MOF) have remained attractive, with their structure and unique optical properties compared to conventional optical fibers. The use of LPG in PCF fibers [2] and hollow-core fibers (HCF) [3] leads to the development of sensors with improved characteristics compared to those based on conventional fibers.

Most of the LPG sensors function in the near IR, which requires expensive detectors. In contrast, the sensors in the visible range [4, 5] make use of cheaper detectors, which reduces the overall cost of the whole system.

Lamps and LEDs used as light sources are either large in size or with a narrow spectrum. Broadband fluorescent sources using organic dyes have been proposed as alternative sources [6-8]. The combination of the spectra of different fluorescence dyes allows an increase of spectral width to cover the visible spectrum. A fluorescence source can easily be integrated with optical fibers, which is an advantage over lamps and LEDs.

In the present paper the authors present a miniature, all-fiber optic fluorescence source compatible with conventional and MOFs. The results presented are a continuation of previous research on the dependence of the fluorescence spectrum on the microcapillary structure filled with a fluorescing dye [9].

A fused silica Polymicro Technologies capillary of 362/100 μm outer/inner diameter was used to hold the active medium. A capillary with a 19mm length was used to hold the fluorescence dye. The polymer coating was removed using Poly super strippa and was further cleaned using ethanol. The capillary was next filled with Rhodamine 6G (R6G), dissolved subsequently in pure ethanol and 99.98% glycerine (0.0002% sulphates, 0.0001% chlorides and 5 ppm heavy metals) as an active medium. The concentration of R6G is 4.10⁻⁴M. The capillaries thus prepared are fixed to a micropositioner having three linear and two angular displacement capabilities. A down taper is placed in one end of the microcapillary to serve as a receiving fiber (RF) for the fluorescence signal. The other end of the fiber is connected to the input of a CCD spectrometer (AvaSpec 2048, Avantes) with a 200 μm entrance slit.

A conventional optical fiber (SMF-28) and two experimental MOFs – a PCF (PIV 070301) and a HCF (Hollow Core) fabricated at the Maria Curie-Skłodowska University in Lublin, Poland were used. The tapers were fabricated using a gas burner and pulled to separation into two parts. Figure 1 shows the general scheme of the optical set-up used for the measurements of all RFs. The capillary probe is side pumped along the active medium using a down-tapered pumping fiber (PF) made of SMF-28 ($\lambda_c=1260\text{nm}$), shown in Fig. 1b. A holder is used to fix it to a single-axis positioner moving orthogonally with respect to the capillary axis. The pumping fiber is excited by a CW DPSS Nd:YAG laser emitting at $\lambda=532\text{nm}$. The capillary is moved along a line in the same plane as the PF using the multi-axis positioner. The output of the PF is curved by the flow of the burner's flame. Fluorescence spectra were taken for four different degrees of contact shown in Fig. 2a). The closest position without direct contact and the increasing degree of contact between the tip of the PF and the capillary are denoted by "0" and "1" through "4".

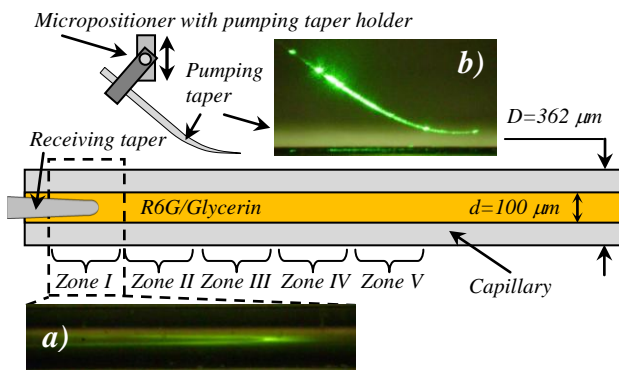


Fig. 1. Experimental set-up with: a) a picture of a tapered RF inserted into a capillary filled with a R6G/Glycerin solution with pump light passing through it for better visualization; b) a picture of a pumping tapered PF which is located near the capillary.

A photograph of the radiation from a PF parallel to the screen is shown in Fig. 2b). The distance from the PF to the screen is $L=11\text{mm}$, $a\approx 17\text{mm}$ and $b\approx 30\text{mm}$.

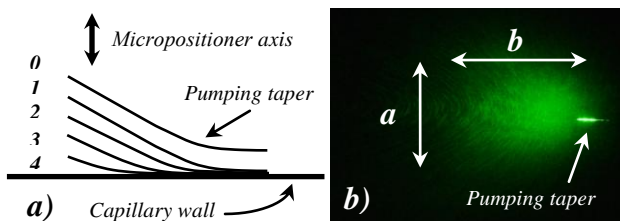


Fig. 2. a) Schematic view of the four increasing degrees (1, 2, 3 and 4) of contact between the PF taper and the capillary in the corresponding irradiated zone. The position in which the PF was located near the capillary without touching it is indicated by "0". b) A picture of the pump spot on a screen.

A conventional $9/125\mu\text{m}$ SMF-28 optical fiber was used to fabricate a receiving taper. Figure 1a) shows a photo of a SMF-28 RF placed in a capillary filled with an active medium with pumping light launched in it to enable visualization. In Figure 1 the five irradiated zones from the capillary for SMF-28 RF are indicated as I, II, III, IV and V. For each zone five (0 to 4) consecutive measurements were taken at a degree of contact between the PF and the capillary (Fig. 2a).

The first experimental MOF used as a RF was a PCF and its end facet electron microscope picture is shown in Fig. 3. It is a fused silica fiber with an outer diameter of $125\mu\text{m}$ and a hexagonal holey structure located in the central area, used as a cladding. In the center of the holey structure a solid section $8\mu\text{m}$ in diameter was placed and used as a core. The pictures of mode spots from PCF on a screen before and after tapering are displayed in Fig. 3 when using pumping light with a wavelength of 532nm . As seen in Fig. 3c), the spot from RF is elliptical in shape, being the result of a curve similar to the one showed in

Fig. 1b). In Figure 3b) $L\approx 35\text{mm}$, the central spot diameter is $d_0\approx 9\text{mm}$, the diameter of the first ring of spots is $d_1\approx 18\text{mm}$. For Fig. 3c) the distance from the fiber to the screen is $L\approx 30\text{mm}$, diameters $a\approx 27\text{mm}$ and $b\approx 36\text{mm}$.

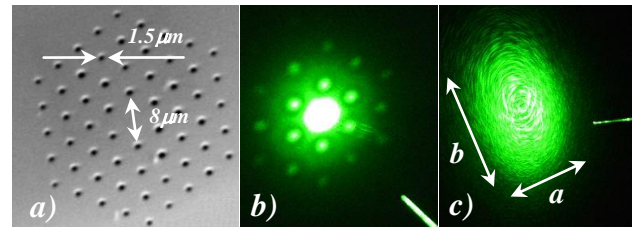


Fig. 3. PCF-based down-taper: a) a cross-section of the PCF taken with a scanning electron microscope, b) far-field pattern from the PCF fiber; c) far-field pattern from the tapered PCF fiber.

The second experimental MOF used as a RF was an HCF whose electron microscope picture of the end facet is shown in Fig. 4. It is an optical fiber made of fused silica with a $125\mu\text{m}$ outer diameter, a $61\mu\text{m}$ diameter central hole and a set of smaller holes located around it. The pictures of far-field patterns from HCF before and after tapering are shown in Fig. 4, for pumping at 532nm . In Fig. 4b) the distance from the fiber to the screen is $L\approx 29.5\text{cm}$, and the diameter is $d\approx 16\text{mm}$. In Figure 4c) the distance from the fiber to the screen is $L\approx 18\text{mm}$, the larger diameter is $D\approx 70\text{mm}$, while the smaller one is $d\approx 17\text{mm}$.

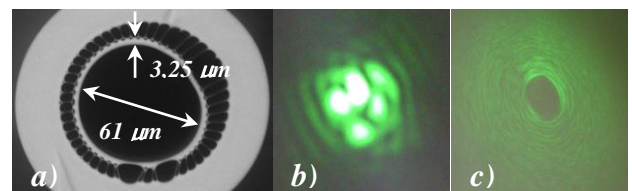


Fig. 4. A picture from an electron microscope of a HCF end facet. Pictures of the mode spots on a screen from HCF a) with a flat end facet before tapering and b) after the tapering.

The deformation of the represented fluorescence spectra which is observed around a wavelength of 630nm is due to a defect in this spectral area of the spectrometer used.

In Figure 5 fluorescence spectra for SMF-28 RF are presented, captured in the irradiated zone II at a corresponding degree of contact, for the integration time $\tau=10\text{ms}$. As seen in Fig. 5a), the intensity of a fluorescent signal increases consistently on increasing the degree of contact. Normalized fluorescent spectra are compared at the maximum degree of contact from each zone in Fig. 5b).

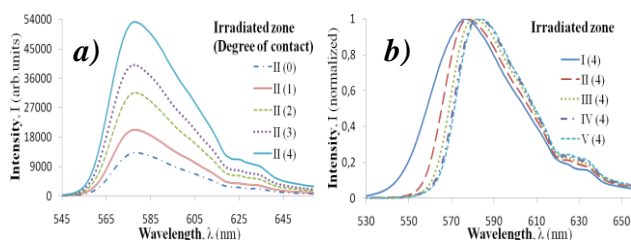


Fig. 5. a) Fluorescence spectra for SMF-28 RF captured in the irradiated zone II. b) Normalized fluorescence spectra from the five irradiated zones at the maximum degree of contact.

The change in spectra width is clearly visible with an increase in the distance from the RF due to its inner filter effect, which is an intrinsic characteristic of organic fluorescent dyes.

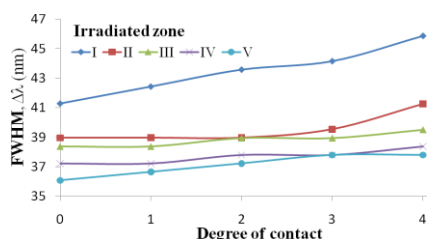


Fig. 6. The change of FWHM depending on degrees of contact for every irradiated zone.

The changes of FWHM of the spectra vs. the degree of contact and irradiation zone are presented in Fig. 6. As it can be seen, the largest FWHM of $\Delta\lambda=45.9\text{nm}$ is observed in zone I at maximum contact. With an increase in the distance from the RF, the FWHM is getting reduced and reaches a value of $\Delta\lambda=37.8\text{nm}$ in zone V at maximum contact. Thus the capillary length can be optimized in order to have a compact light source as a result.

The normalized fluorescent spectra captured with PCF and HCF RFs after the irradiation of the relevant zones and the respective degrees of contact are presented respectively in Figs. 7a) and b). The spectra were captured at the integration time $\tau=50\text{ms}$ (PCF RF) and $\tau=100\text{ms}$ (HCF RF). As seen, the change of the normalized spectra for PCF RF is similar to that of SMF-28 RF. The data for the FWHM change vs. the degree of contact with an increasing distance from the RF show a logical tendency for the FWHM narrowing. As in the case of SMF-28 RF, the highest FWHM value of $\Delta\lambda=42.5\text{nm}$ is observed at irradiation near the tip of the RF, at a maximum degree of contact. Because the HCF diameter is slightly over $125\mu\text{m}$ and a standard coupler cannot be used, the signal from the HCF RF is received via $200\mu\text{m}$ fibre positioned at the tip of the HCF RF connected to the spectrometer. The narrowing of the FWHM with an increase in the distance from the RF is seen again. In this case a FWHM of

$\Delta\lambda=37.3\text{nm}$ is observed at irradiation with a maximum degree of contact in zone I.

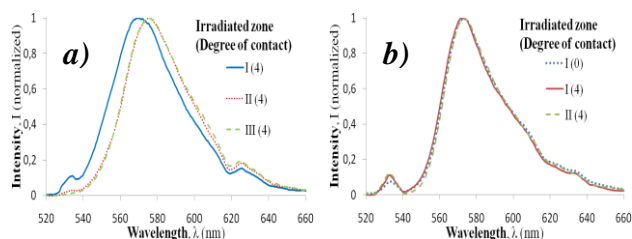


Fig. 7. Normalized fluorescence spectra captured with a) PCF RF and b) HCF RF.

A miniature all-fiber fluorescent source based on organic dyes, compatible with convectional and MOFs is demonstrated. The capillary tubes used in combination with the tapered RF are stable, cheap and easy to assemble into an integrated structure. The scheme of side irradiation via tapered optical fiber allows the construction to be more compact and stable. Moreover, it would allow the placement of additional capillaries filled with an active medium symmetrically located around the tapered optical fiber. This would allow more efficient use of the pumping light. The experimental data show that the highest spectral width $\Delta\lambda=45\text{nm}$ (SMF-28), $\Delta\lambda=42.5\text{nm}$ (PCF), $\Delta\lambda=37.3\text{nm}$ (HCF), is seen at irradiation near the tip of the tapered RFs. Also two different sensors can be powered by a common light source. On the basis of the presented fluorescent source, disposable sensors can be developed and be suitable for field measurements.

Support for this work by the Internal Research Funding under grant FF003 of the Plovdiv University is gratefully acknowledged.

References

- [1] S. James, R. Tatam, Meas. Sci. Technol. **14**(5), R49 (2003).
- [2] Y.P. Wang, L. Xiao, D. Wang, W. Jin, Opt. Lett. **31**(23), 3414 (2006).
- [3] Y. Wang, W. Jin, J. Ju, H. Xuan, H. Ho, L. Xiao, D. Wang, Opt. Exp. **16**(4), 2784 (2008).
- [4] L. Rindorf, O. Bang, Opt. Lett. **33**(6), 563 (2008).
- [5] G. Durana, J. Gomez, G. Aldabaldetrek, J. Zubia, A. Montero, I. Saez de Ocariz, IEEE Sens. J. **12**(8), 2668 (2012).
- [6] D. Vezenov, B. Mayers, D. Wolfe, G. Whitesides, App. Phys. Lett. **86**(4), 041104 (2005).
- [7] B. Mayers, D. Vezenov, V. Vullev, G. Whitesides, Anal. Chem. **77**(5), 1310 (2005).
- [8] J.-M. Lim, S.-H. Kim, J.-H. Choi, S.-M. Yang, Lab Chip **8**(9), 1580 (2008).
- [9] V. Vladev, T. Eftimov, Union of Scientists in Bulgaria-Plovdiv **16**, 73 (2014).